Mechanical Properties and Failure Surface Morphology of Amine-Cured Epoxy/Clay Nanocomposites

Hiroaki Miyagawa,[1] Kit H. Foo,[2] Isaac M. Daniel,[3] Lawrence T. Drzal[1]

[1]*Composite Materials and Structures Center, Michigan State University, East Lansing, Michigan 48824-1226*
[2]*Department of Chemical Engineering and Material Science, University of California at Davis, Davis, California 95616*
[3]*Center for Intelligent Processing of Composites, Northwestern University, Evanston, Illinois 60208*

Received 20 April 2004; accepted 24 August 2004
DOI 10.1002/app.21357
Published online in Wiley InterScience (www.interscience.wiley.com).

ABSTRACT: The tensile and impact properties of amine-cured diglycidyl ether of bisphenol A based nanocomposites reinforced by organomontmorillonite clay nanoplatelets are reported. The sonication processing scheme involved the sonication of the constituent materials in a solvent followed by solvent extraction to generate nanocomposites with homogeneous dispersions of the organoclay nanoplatelets. The microstructure of the clay nanoplatelets in the nanocomposites was observed with transmission electron microscopy, and the clay nanoplatelets were well dispersed and were intercalated and exfoliated. The tensile modulus of epoxy at room temperature, which was above the glass-transition temperature of the nanocomposites, increased approximately 50% with the addition of 10 wt % (6.0 vol %) clay nanoplatelets. The reinforcing effect of the organoclay nanoplatelets was examined with respect to the Tandon–Weng and Halpin–Tsai models. The tensile strength was improved only when 2.5 wt % clay nanoplatelets were added. The Izod impact strength decreased with increasing clay content. The failure surfaces of the nanocomposites were observed with environmental scanning electron microscopy and confocal laser scanning microscopy. The roughness of the failure surface was correlated with the tensile strength. J Appl Polym Sci 96: 281–287, 2005

Key words: microstructure; modulus; nanocomposites; organoclay; strength

INTRODUCTION

The usefulness of exfoliated smectite clay nanoplatelets as reinforcements in organic polymers has been well reported over the past decade.[1] Previous studies have documented the processing, mechanical, and thermal characteristics of epoxy/clay nanocomposites. The Pinnavaia group reported improved tensile strength and modulus in amine-cured rubbery epoxy[2–4] and glassy epoxy[3–6] nanocomposites. Improvements in the dimensional stability,[6] heat distortion temperature, and flammability resistance[7] have also been reported for organoclay/amine-cured epoxy nanocomposites. Some authors have already reported that anhydride-cured epoxy/clay nanocomposites have been processed, and the Tandon–Weng[8] equations have been useful for evaluating the reinforcing effect on the storage modulus measured by dynamic mechanical analysis (DMA).[9] In a previous study, a pseudo-inclusion model was proposed to adapt these equations, to intercalated clay nanocomposites, in which individual clay nanoplatelets were inhomogeneously dispersed. A pseudo-inclusion model enabled to apply Tandon-Weng equations to the intercalated clay nanocomposites, although these equations assumed that the reinforcements were homogeneously dispersed.

In this study, nanocomposites composed of amine-cured diglycidyl ether of bisphenol A (DGEBA) reinforced with organomontmorillonite clay nanoplatelets were processed by sonication, and their tensile and impact properties are reported. The microstructure of the clay nanoplatelets was observed with transmission electron microscopy (TEM). The reinforcing effect of the organoclay nanoplatelets on the tensile modulus (E) is discussed with respect to the Tandon–Weng and Halpin–Tsai models. The morphology of the failure surfaces of the nanocomposites was examined with environmental scanning electron microscopy (ESEM) and confocal laser scanning microscopy (CLSM). Finally, the roughness of the failure surface was correlated with the tensile strength.

EXPERIMENTAL

Materials

In this study, the epoxy resin was DGEBA (DER 331; epoxide equivalent weight = 187) processed with the

Correspondence to: H. Miyagawa (miyagaw2@egr.msu.edu).

Contract grant sponsor: University of Utah (as part of a U.S. Department of Energy contract entitled "A Multiscale Modeling and Experimental Study of the Mechanics of Polymer Nanocomposite Materials"); contract grant number: 2103050.

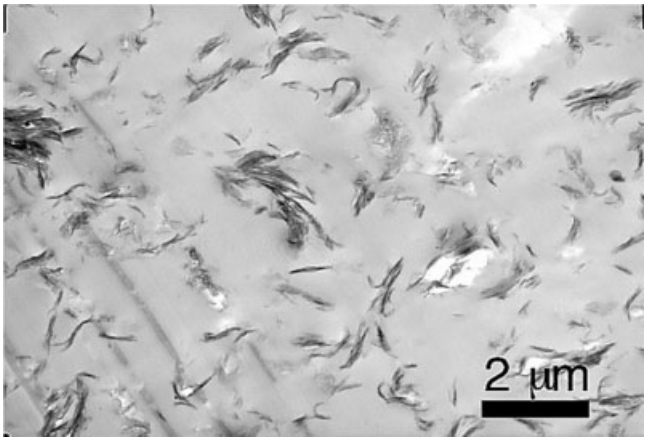

Figure 1 Low-magnification TEM micrograph revealing the dispersion of clay nanoplatelets at a 7.5 wt % (4.5 vol%) loading.

reactive diluent poly(glycol diepoxide) (DER732; epoxide equivalent weights = 320) and triethylene tetramine (DEH 24; equivalent weight = 24.4; all from Dow Chemical Co., Midland, MI). The DER331/DER732/DEH24 mixing ratio was 70:30:11 (w/w/w). The nanocomposites were made with Cloisite 30B (Southern Clay Products, Gonzales, TX), a natural montmorillonite modified with methyl, tallow, and bis(2-hydroxyethyl) (MT2EtOH) quaternary ammonium salt. The first step was to sonicate the clay in a liquid that was a suitable solvent for the epoxy resin system used in this study. Because of its low boiling point, which facilitated easy extraction from the blend, acetone was selected as the solvent to mix the constituents. To fabricate the nanocomposites, the clay was sonicated in acetone for an hour with a solution concentration of approximately 30 L of acetone/kg of clay. The epoxy resin and the reactive diluent were then added, and the blend was mixed with a magnetic stirrer for an additional hour. The acetone was removed by vacuum extraction at 100°C for 24 h, after which time the amine curing agent was blended into the solution with a magnetic stirrer. All the specimens were cured at room temperature for 16 h and postcured at 100°C for 3 h.

TEM

The exfoliated/intercalated clay nanolayers in the amine-cured epoxy nanocomposites were observed with TEM. Thin sections (ca. 70 nm) were collected at room temperature with an RMC 7 ultramicrotome (Boeckeler Instruments Inc., Tucson, AZ) fitted with a diamond knife having an included angle of 4°. The TEM micrographs were collected with a JEOL 100CX TEM instrument (JEOL Ltd., Tokyo, Japan) with an LaB_6 filament operating at a 120-kV accelerating voltage.

Tensile testing

Tensile testing was conducted to measure *E*, Poisson's ratio, the tensile strength, and the ultimate strain at failure for both amine-cured neat epoxy and its clay nanocomposites with different clay loadings. The experiments were performed at a crosshead velocity of 0.38 mm/min (0.015 in/min). At least five specimens for each composition were tested.

Izod pendulum impact resistance

The Izod impact strength was measured for neat epoxy and epoxy/clay nanocomposites at room temperature. Izod impact specimens with the same dimensions as indicated in ASTM D 256 standard were tested with a 453-g (1.0-lb) pendulum. At least four specimens for each composition were tested to reduce scattering error.

Fractographic observations

The failure surfaces of tensile specimens were observed with a Philips ElectroScan 2020 environmental scanning electron microscope (FEI Company, Acht, The Netherlands) at a 20-kV accelerating voltage after the failure surfaces were coated with thin Au films. A Zeiss LSM 210 confocal laser scanning microscope (Carl Zeiss AG, Jena, Germany) was used to acquire three-dimensional surface topography of failure surfaces for the evaluation of the failure surface roughness. A 50× lens at a zoom of 50× produced a field size of approximately 120 μm × 80 μm. At least 10 topography images were acquired for each different composition at a random location near the center of the specimen failure surfaces that was far enough from the specimen edges. All images were filtered to

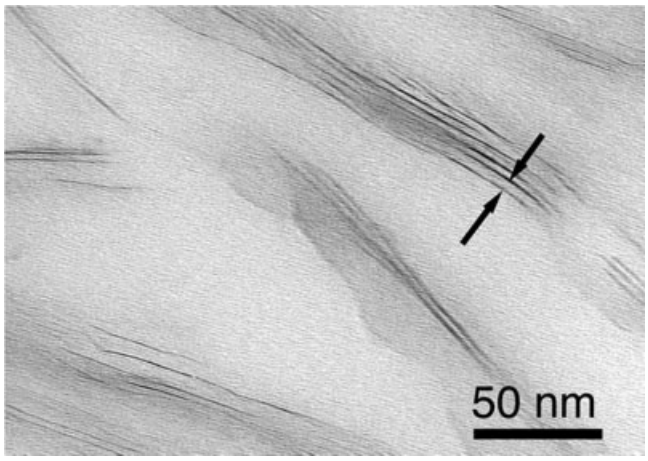

Figure 2 High-magnification TEM micrograph revealing well-intercalated/expanded clay nanolayers in an amine-cured epoxy matrix at a 7.5 wt % loading.

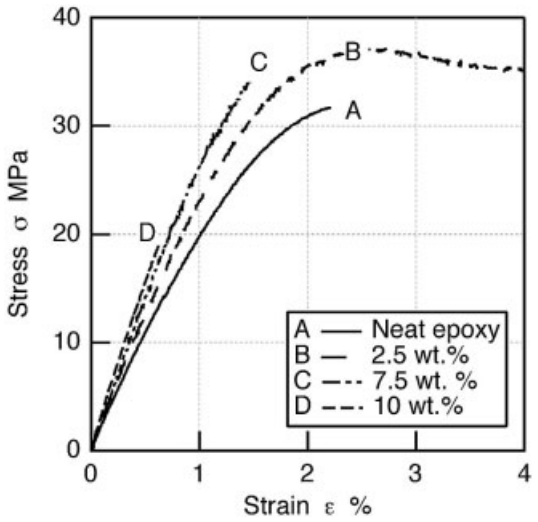

Figure 3 Stress (σ)–strain (ε) curves of neat epoxy and its clay nanocomposites.

reduce noise and then adjusted with tilt correction to evaluate the arithmetic mean deviation (R_a) of the failure surface profile.

RESULTS AND DISCUSSION

Clay dispersion morphology

Figure 1 is a low-magnification TEM micrograph at a 7.5 wt % (4.5 vol%) clay loading, showing a representative region of the dispersed clay nanoplatelets in the epoxy resin. The specimen contained both clusters of clay and exfoliated clay nanoplatelets. In general, the dispersion of the clay was uniform.

The detailed features of the exfoliated/intercalated clay nanoplatelets for a 7.5 wt % nanocomposite are shown in the bright-field TEM micrograph of Figure 2. The view perpendicular to the *c* axis (i.e., along the *a*–*b* plane) shows a typical elongated, fiberlike feature of the clay nanoplatelets. The basal spacing of the clay nanoplatelets in the epoxy matrix can be clearly distinguished. The *d*-spacing of the organomontmorillonite clay was 1.80 nm according to X-ray diffraction before sonication in acetone. From Figure 2, the expanded clay *d*-spacing in the amine-cured epoxy system was measured to be 4.32 nm. This larger *d*-spacing, in comparison with the original *d*-spacing of the organoclay, indicated that the polymer network intercalated between the clay basal layers.

Mechanical properties of the clay nanocomposites

Typical examples of the stress–strain curves of amine-cured neat epoxy and its clay nanocomposites with different clay loadings are shown in Figure 3. Generally, an amine-cured epoxy is softer than an anhydride-cured epoxy. Because the reactive diluent was added to DGEBA and cured with an amine curing agent, the neat epoxy was relatively soft, and consequently, plastic behavior is clearly observable in the stress–strain curve. After the addition of 2.5 wt % (1.5 vol %) clay nanoplatelets, plastic behavior was quite evident, although the nanocomposites became more elastic for the 5.0–10 wt % (3.0–6.0 vol %) clay loadings. Furthermore, *E* increased with increasing clay content.

Figure 4 shows the change in *E* of the amine-cured neat epoxy and its clay nanocomposites as a function of the clay volume fraction (V_c) at room temperature. For 10 wt % clay nanocomposites, *E* improved 50% with respect to the neat epoxy. The solid line in Figure 4 is the least-squares regression fit to the experimental results. Some authors[9] have evaluated the reinforcing effect of clay nanoplatelets on the storage modulus measured by DMA with the Tandon–Weng equations for two-dimensional and three-dimensional randomly oriented composites. The storage modulus was also calculated with the Halpin–Tsai equation,[10] which was used to evaluate unidirectional fiber-reinforced composites. The following equations were used:

$$E_L = E_m \frac{1 + \eta_L \xi V_c}{1 - \eta_L V_c} \quad (1)$$

$$E_T = E_m \frac{1 + 2\eta_T V_c}{1 - \eta_T V_c} \quad (2)$$

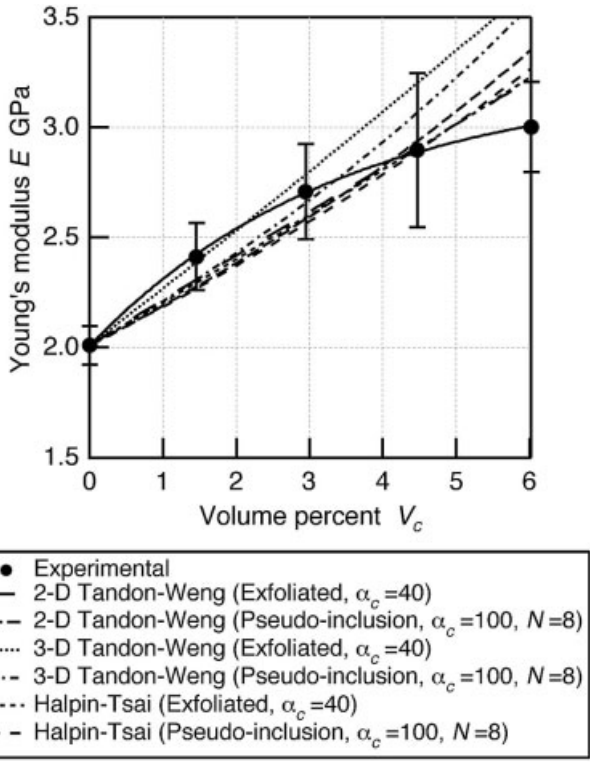

Figure 4 Improvement in *E* of amine-cured epoxy/clay nanocomposites with changes in the clay content.

where

$$\eta_L = \frac{\frac{E_c}{E_m} - 1}{\frac{E_c}{E_m} + \zeta} \tag{3}$$

$$\eta_T = \frac{\frac{E_c}{E_m} - 1}{\frac{E_c}{E_m} + 2} \tag{4}$$

E and V refer to the elastic modulus and volume fraction, respectively. The subscripts L, T, m, and c refer to the longitudinal property, transverse property, matrix property, and clay property, respectively. van Es[11] proposed the following parameter:

$$\zeta = 2\alpha_c/3 = 2l_c/3t_c \tag{5}$$

where α_c, l_c, and t_c refer to the aspect ratio, length, and thickness of the exfoliated clay nanoplatelets. Because of the redefinition in eq. (5), an evaluation with the Halpin–Tsai equation was almost the same as one with the two-dimensional Tandon–Weng equation. Finally, the elastic modulus of randomly oriented nanocomposites (E_n) was obtained as follows:

$$E_n = \frac{3}{8} E_L + \frac{5}{8} E_T \tag{6}$$

For the E values shown in Figure 4, the values from three different equations calculated with the same value of α_c (40) are plotted as three different segmented lines. In this evaluation, the clay nanoplatelets were regarded as completely exfoliated. Although all three equations fit the experimental data reasonably with $\alpha_c = 40$, the assumed aspect ratio was much shorter than the actual aspect ratio of clay nanoplatelets measured by TEM. The Tandon–Weng and Halpin–Tsai models assume uniformly dispersed platelets, but the clay nanoplatelets were variable in size and were inhomogeneously dispersed in the epoxy matrix, as shown in Figure 1. Thus, the nonuniform dispersion and intercalation of the resin in the nanoclay galleries were not explained in the Tanden–Weng scheme, which produced errors in the evaluation of the aspect ratio of clay nanoplatelets.

To overcome errors from the existence of the intercalated clay nanoplatelets in the theoretical evaluation, Brune and Bicerano[12] applied a pseudo-inclusion concept with the Halpin–Tsai equation for intercalated clay that was unidirectionally aligned in a nanocomposite. This pseudo-inclusion model could also be applied to randomly oriented clay nanocomposites with not only the Halpin–Tsai equation but also the Tandon–Weng equation. The d-spacing of the intercalated clay nanoplatelets determined with TEM, 4.3 nm, was used for the calculations of the pseudo-inclusion properties. With the pseudo-inclusion properties, the Tandon–Weng and Halpin–Tsai equations were used to calculate the storage modulus of intercalated clay nanocomposites. Figure 4 also shows the results of the Tandon–Weng and Halpin–Tsai schemes with the pseudo-inclusion model. With a sensitivity approach, the number of intercalated layers (N) and the aspect ratio of the pseudo-inclusion could be estimated. The predictions from the pseudo-inclusion model shown in Figure 4 were computed with $N = 8$ and $\alpha_c = 100$, yielding a close fit to the experimental data. Other combinations of N and α_c also resulted in a good prediction of the nanocomposites modulus.

There was a qualitative difference between the theories and the experimental results that was evidenced by the different trends. In Figure 4, all theoretical predictions are upward, whereas the experimental results level off. The theoretical equations show that the composite modulus increased with increasing volume from the matrix modulus to the filler modulus. However, there is actually an upper limit for the improvement of the composite modulus. This implies that the theoretical evaluation is realistic only within a small volume. Indeed, in this study, the epoxy showed an extremely viscous nature with 6.0 vol % (10 wt %) clay, even though the low-viscous reactive diluent was used to process epoxy nanocomposites, and so it was difficult to mix the epoxy/clay blend with the amine curing agent. The trend in Figure 4 shows that the composite modulus did not exceed 3.5 GPa with more than 6.0 vol % clay.

Figure 5 shows the experimental results of the tensile strength of the amine-cured neat epoxy and its nanocomposites with different clay loadings. An improvement in the tensile strength was only observed for a clay loading of 2.5 wt %. For clay loadings exceeding 5.0 wt %, the tensile strength radically decreased and reached a constant value. Lan and Pinnavaia[2] reported excellent improvement of the tensile strength of amine-cured rubbery epoxy, which had a lower glass-transition temperature than room temperature, with the addition of clay nanoplatelets. This suggests that the tensile strength is improved when the matrix of nanocomposites is a soft epoxy material showing large plasticity. In fact, the amine-cured neat epoxy shows a clear plastic behavior in the stress–strain curve in Figure 5, and even greater plastic behavior was observed for 2.5 wt % clay nanocomposites. However, when more than 5.0 wt % clay was added to the amine-cured epoxy, the nanocomposites became more brittle and showed little plastic behavior in the stress–strain curve. For conventional particle-reinforced plastics, lower tensile strength was ob-

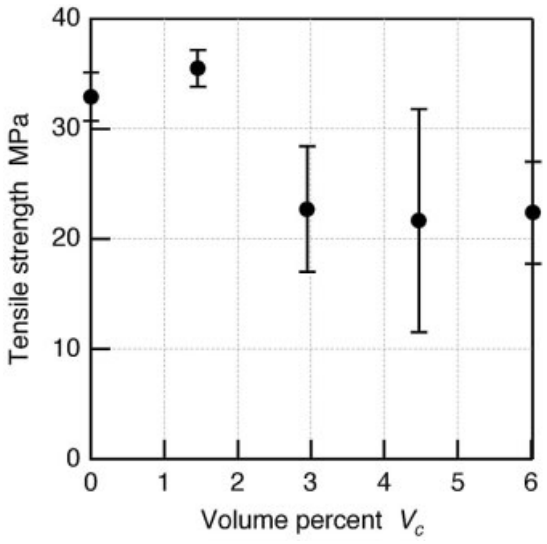

Figure 5 Change in the tensile strength of amine-cured epoxy nanocomposites with changes in the clay content.

tained when the reinforcements were not homogeneously dispersed. Therefore, it is possible that the existence of intercalated clay nanoplatelets may result in the lower tensile strength.

Figure 6 shows the change in the ultimate strain at failure with different clay contents. The ultimate strain reached a maximum at a clay loading of 2.5 wt %. Although only a small improvement in the tensile strength was observed for 2.5 wt % clay nanocomposites, the improvement in the ultimate strain was 18%. This was due to the larger plastic deformation with 2.5 wt % clay under a tensile loading. At higher clay loadings, the ultimate strain radically decreased and reached a constant value, as observed with the tensile strength, because of the lack of plastic behavior under tensile loading. Therefore, the results in Figures 4–6 suggest that maintaining plastic deformation is an important factor in improving the tensile strength.

Figure 7 shows the relation between the Izod impact strength and clay content in an amine-cured epoxy matrix. The strength radically decreased more than 50% when up to 5.0 wt % clay nanoplatelets were added, and then the strength decreased to a constant value. With a clay loading of 5.0–10 wt %, less plastic behavior was observed in the stress–strain curve, and this implied that the nanocomposites were more rigid than the neat epoxy. As a result, the Izod impact strength decreased with the addition of clay nanoplatelets. Some authors have already reported that the Izod impact strength of anhydride-cured epoxy is reduced with the addition of clay nanoplatelets.[13] It has also been reported that the addition of silica nanoparticles results in the improvement of the Izod impact strength of both amine- and anhydride-cured epoxies.[14] Therefore, it can be concluded that clay nanoplatelets are not suitable for improving the Izod impact strength, although they do improve the elastic modulus because of the large aspect ratio.

Fractographic observations

Failure surface morphologies were observed by ESEM at an arbitrary location near the center of the specimen failure surfaces that was far enough from the specimen edges. Figure 8 shows the different morphologies of the failure surfaces for amine-cured neat epoxy and its nanocomposites with 2.5 wt % clay. The failure surface of the neat epoxy shown in Figure 8(a) was

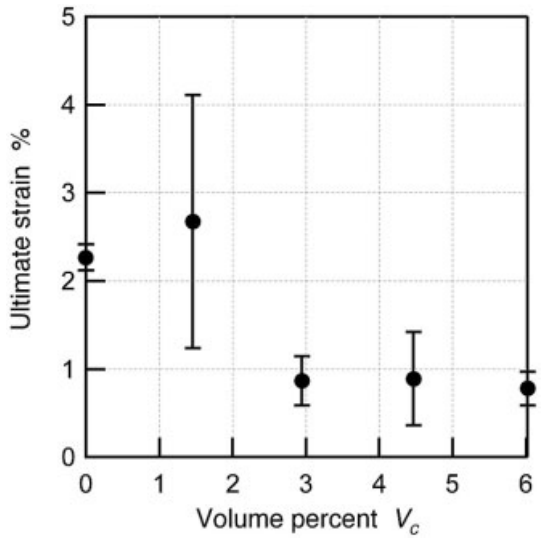

Figure 6 Change in the ultimate strain of amine-cured epoxy nanocomposites with changes in the clay content.

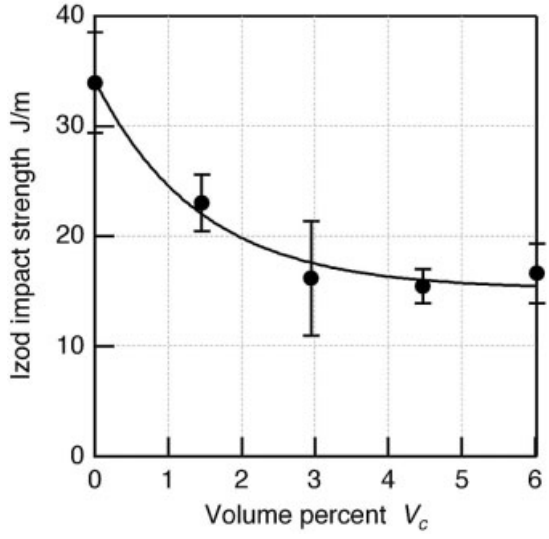

Figure 7 Change in the Izod impact strength of amine-cured epoxy/clay nanocomposites with changes in the clay content.

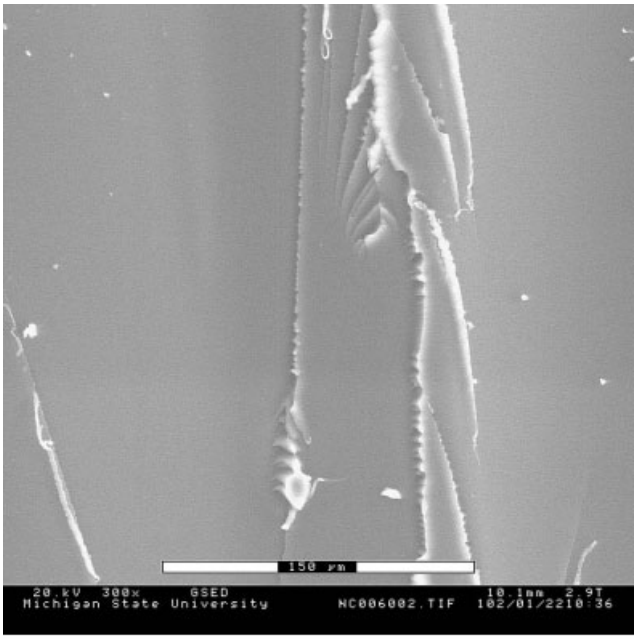

(a)

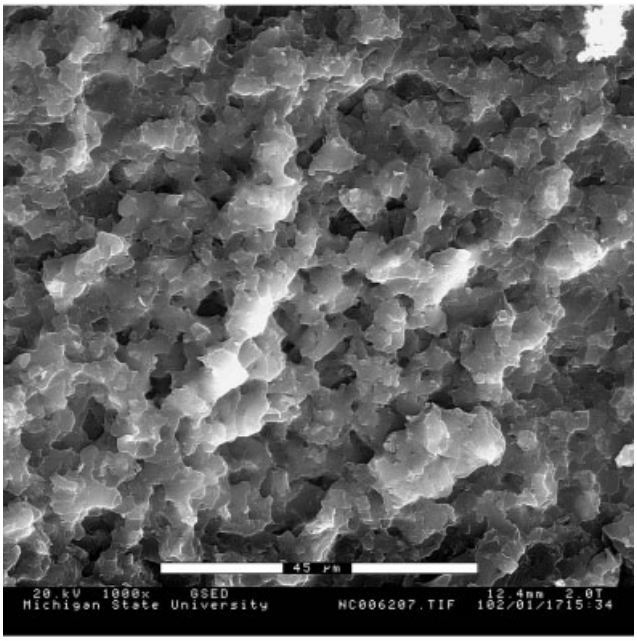

(b)

Figure 8 ESEM micrographs of tensile failure surfaces: (a) amine-cured epoxy (original magnification = 300×; scale bar = 150 μm) and (b) 2.5 wt % clay nanocomposites (original magnification = 1000×; scale bar = 45 μm)

extremely flat. The failure surface of the clay nanocomposites shown in Figure 8(b) was much rougher than that of the neat epoxy. It has been reported that the fracture surfaces of clay nanocomposites are flat like that in Figure 8(a) when clay nanoplatelets are not chemically modified and thus the bonding at the clay/epoxy interface is poor.[13] Therefore, Figure 8(b) suggests the excellent bonding condition at the epoxy/clay interface because of the clay modification with MT2EtOH.

CLSM is a useful method for quantifying the surface roughness, which can be correlated with the tensile strength. To analyze R_a and the maximum height, we conducted topographic measurements of failure surfaces for all samples at an arbitrary location near the center of the specimen failure surfaces that was far enough from the specimen edges, as shown in Figure 9. The epoxy matrix and the clay nanoplatelet had different elastic moduli, and so the stress concentration occurred at the epoxy/clay interfaces. Moreover, the adhesion at the epoxy/clay interfaces was often

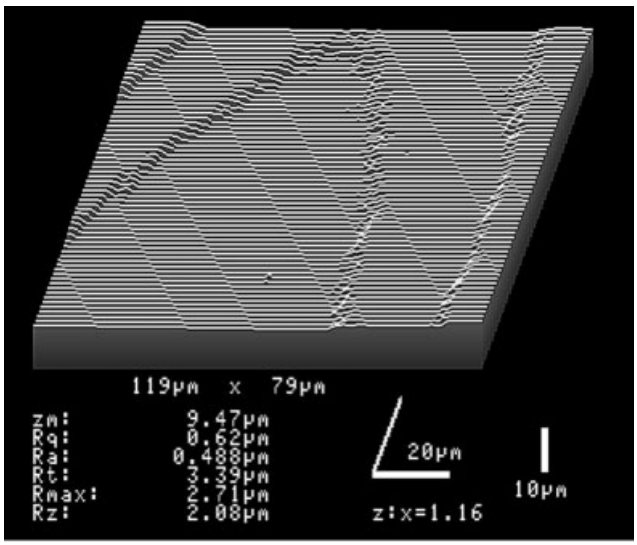

(a)

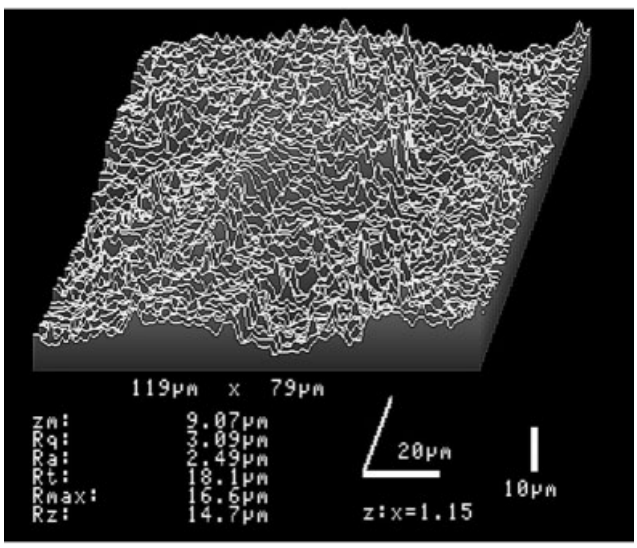

(b)

Figure 9 Three-dimensional topography measurements of the tensile failure surfaces: (a) amine-cured epoxy and (b) 2.5 wt % clay nanocomposites.

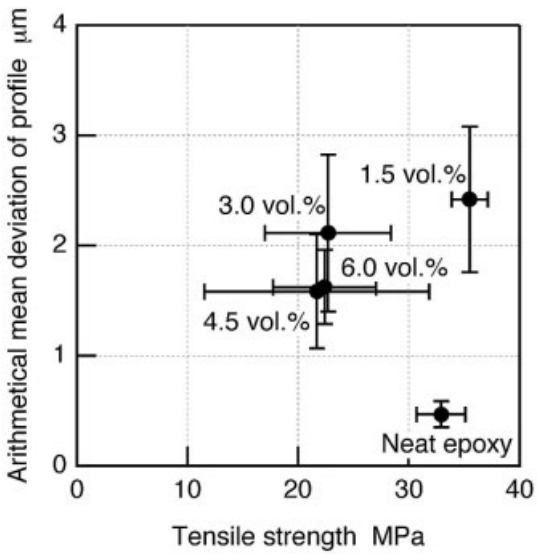

Figure 10 Relation between the tensile strength and roughness of the tensile failure surface for amine-cured nanocomposites.

imperfect. Consequently, the nano-order defects definitely existed in the epoxy/clay nanocomposites under tensile loading. When small defects are regarded as cracks, the change in the tensile strength for elastic materials can be explained by Griffith's theory,[15] in which the crack is propagated when the strain energy is released to create a new fracture surface. Hence, when the fracture surface area is larger, more released strain energy is necessary. Consequently, the failure surface area is larger when the tensile strength of nanocomposites is improved.

Figure 10 shows the correlation between R_a and the tensile strength. From Griffith's theory,[15] a correlation was observed for only epoxy nanocomposites with different clay loadings. The tensile strength was dependent not only on the surface roughness but also on the adhesion at the epoxy/clay interface. Because there was no epoxy/clay interface, the failure surface of the amine-cured neat epoxy was still flat (as observed by ESEM), although it already had excellent tensile strength. Therefore, the values of the failure surface roughness and the tensile strength of amine-cured neat epoxy could not be correlated with the values of the epoxy/clay nanocomposites.

CONCLUSIONS

Nanocomposites composed of amine-cured DGEBA reinforced with organomontmorillonite clay nanoplatelets were processed by sonication, and their tensile and impact properties were examined. It was observed by TEM that the *d*-spacing of clay nanoplatelets in the epoxy matrix was expanded to 4.32 nm after the fabrication. *E* of epoxy at room temperature, which was above the glass-transition temperature of the nanocomposites, increased approximately 50% with the addition of 10 wt % (6.0 vol %) clay nanoplatelets, with respect to the value of unfilled epoxy. The reinforcing effect of the organoclay nanoplatelets on *E* was evaluated with respect to the Tandon–Weng and the Halpin–Tsai models, and the theoretical values fit the experimental results with the pseudo-inclusion model. The tensile strength was improved only when 2.5 wt % (1.5 vol %) clay nanoplatelets were added to the amine-cured epoxy because of the large plastic behavior. The Izod impact strength radically decreased with an increasing amount of the clay nanoplatelets. The morphology of the failure surfaces of the nanocomposites was observed with ESEM and CLSM. The roughness of the failure surface was correlated with the tensile strength.

The authors acknowledge samples provided by Southern Clay Products, Inc. (Gonzales, TX), and Dow Chemicals Co. (Midland, MI).

References

1. LeBaron, P. C.; Wang, Z.; Pinnavaia, T. J. Appl Clay Sci 1999, 15, 11.
2. Lan, T.; Pinnavaia, T. J. Chem Mater 1994, 6, 2216.
3. Pinnavaia, T. J.; Lan, T.; Wang, Z.; Shi, H. Z.; Kaviratna, P. D. In Nanotechnology Molecularly Designed Materials; ACS Symposium Series 622; Chow, G.-M.; Gonsalves, K. E., Eds.; American Chemical Society: Washington, DC, 1996; p 250.
4. Wang, Z.; Lan, T.; Pinnavaia, T. J. Chem Mater 1996, 8, 2200.
5. Lan, T.; Kaviratna, P. D.; Pinnavaia, T. J. Chem Mater 1995, 7, 2144.
6. Massam, J.; Pinnavaia, T. J. Mater Res Soc Symp Proc 1998, 520, 223.
7. Brown, J. M.; Curliss, D.; Vaia, R. A. Chem Mater 2000, 12, 3376.
8. Tandon, G. P.; Weng, G. J. Compos Sci Technol 1986, 27, 111.
9. Miyagawa, H.; Rich, M. J.; Drzal, L. T. Polym Compos, to appear.
10. Halpin, J. C.; Tsai, S. W. Air Force Technical Report AFML-TR 67-423; Wright Aeronautical Labs: Dayton, OH, 1967.
11. van Es, M. Ph.D. Thesis, University of Delft, 2002.
12. Brune, D. A.; Bicerano, J. Polymer 2002, 43, 369.
13. Miyagawa, H.; Drzal, L. T. J Adhesion Sci Technol 2004, 18, 1571.
14. Miyagawa, H.; Rich, M. J.; Drzal, L. T. 31st Annual Conference of the North American Thermal Analysis Society, Albuquerque, NM, 2003 [CD-ROM]; North American Thermal Analysis Society: Albuquerque, NM, 2003; 109.
15. Griffith, A. A. Philos Trans R Soc Ser A 1920, 221, 163.